Journal of Engineering Science and Technology
Special Issue on SOMCHE 2014 & RSCE 2014 Conference, January (2015) 48 - 61

POLYPROPYLENE PRODUCTION SIMULATION WITH CAPE-OPEN INTERFACING OF PRO/II AND gPROMS

J. C. LEE[1], O. S. KOFI[2], S. H. KIM[2], S. U. HONG[2], M. OH.[2,*]

[1]Schneider-electric Co., Ltd., 13F, Jei Platz, 186, Digital 1st, Geumcheon-gu, Seoul, Korea
[2] Dept. of Chemical & Biological Engineering, Hanbat National University,
Daejeon 305-719, Korea
*Corresponding Author: minoh@hanbat.ac.kr

Abstract

A dynamic pseudo-homogeneous model was made expressing liquid-phase homo-propylene polymerisation in a stirred reactor with reaction kinetics based on the Ziegler-Natta catalyst. An energy balance was made to analyse heat management in this exothermic reaction. The model was simulated using gPROMS process software and validated with a reference paper to ensure the model's reliability. Results of the simulation and the reference agreed with a reasonable degree of error. The method of moments was employed to predict the average molecular weights and the polydispersity and melt flow indices. Meanwhile, models for the separation and treatment of the polymer formed were formulated using PRO/II software. Consequently, the steady state form of model from gPROMS was connected by CAPE-OPEN interface to PRO/II modelling environment. The flowsheet from this multi-scale modelling approach was simulated with industrial data. It is concluded, this approach enables the multi-scale plant simulation for various equipment and rigorous reactor models simultaneously, without much modelling efforts while we maintain accuracies at reduced computational cost.

Keywords: Homo-polymerisation, Spheripol process, Polymer properties, Multi-scale modelling, CAPE-OPEN.

1. Introduction

Polypropylene is one of the most widespread polymers that has found its daily usage in many applications for domestic and commercial areas. The use of mathematical models to study and analyse chemical industrial processes is common as it affords us the privilege to predict the behaviour of the process.

Fundamentally, a rigorous polymerisation process model, which expresses the

Nomenclatures

A	Heat transfer surface area, m^2
AlR_3	Triethylaluminium concentration, mol/L
C^*	Catalyst active site concentration, mol/L
C_d	Deactivated site concentration, mol/L
C_p	Specific heat capacity, J/kg-K
E	Activation energy, J/mol
E_f	Flexural modulus, GPa
f	Mass flow rate, kg/h
i	Number of chains
k_{im}	Monomer initiation rate constant, L/mol-s
k_p	Chain propagation rate constant, L/mol-s
k_{trA}	Chain transfer to AIR_3 rate constant, L/mol-s
k_{trH}	Chain transfer to hydrogen rate constant, L/mol-s
k_{trm}	Chain transfer to monomer rate constant, L/mol-s
k_d	Chain deactivation constant, s^{-1}
M	Monomer concentration, mol/L
m_0	Monomer molecular weight, g/mol
Max_{CL}	Maximum chain length number
$\bar{M}_N$	Number average molecular weight, g/mol
$\bar{M}_W$	Weight average molecular weight, g/mol
NO_{SI}	Number of sub-intervals
P_i*	Live polymer of i number of chains, mol/L
P_i	Dead polymer of i number of chains, mol/L
q^{in}	Inlet volumetric flow rate, L/s
q	Outlet volumetric flow rate, L/s
r_p	Rate of polymerisation, mol/L-s
S^e	Energy generation source term, J/s
S^m	Mass source generation term, mol/L-s
T	Temperature, ^oC
T^j	Temperature of Jacket, ^oC
U	Heat transfer coefficient, W/m^2-K
V_R	Volume of reactor, L

Greek Symbols

ϕ	Reaction species
λ_k^*	k^{th} moment of live polymer chain
λ_k	k^{th} moment of dead polymer chain
ρ_s	Density of slurry mixture
ΔH_r	Heat of polymerisation, J/mol

Abbreviations

MFI	Melt Flow Index, g/10min
MW	Molecular Weight, g/mol
PDI	Polydispersity Index

physical and thermodynamic properties, material and energy balances and polymerisation kinetics, is crucial for exploring and evaluating changes in feed composition and operation conditions.

The modelling of the polymerisation process in available publications generally, focuses on aspects like, reactor modelling, polymerisation mechanism and molecular weight distribution, as well as, polymer property calculations. The advantages of liquid phase loop reactors are first recognised as being their capabilities to promote high mixing of reactants in the reaction vessel and to allow for high heat transfer rates with the cooling jacket due to their high heat transfer area [1]. Similarly, Zacca and Ray [2] modelled loop reactors as two tubular sections interconnected by perfectly mixed inlet and outlet zones. Again they demonstrated that at high recycle ratios, the loop reactor can be modelled as CSTR as there is perfect mixing of material.

The implications of this assumption meant that all state variables (e.g., temperature, pressure, slurry density) in the reactors are uniform and change only with polymerisation time [3]. Further corroborations were also done to confirm the earlier suggestions that the residence time distribution of the tubular loop reactors under these fast cycling conditions resemble that of the CSTR [4].

Whilst most publications focus on either reactor modelling or kinetic mechanisms of polymerisation, not much has been done on the modelling of the entire polypropylene production process on the multi-scale level. In this work, a multi-scale simulation of polypropylene production was executed in two software packages (gPROMS [5]/ PRO/II [6]) connected in the framework of CAPE-OPEN. The polypropylene production process is described in section 2. This is followed by the elucidation of the modelling topology and the reactor model in section 3. Section 4 states and discusses the results of the simulation whilst conclusions for the work are stated in Section 5.

2. Process Description

In the present study, the Spheripol loop technology [7], which involves the continuous loop reactors at the centre is studied. The Spheripol process is a modular technology consisting of three main process steps – catalyst and raw material feeding, polymerisation and finishing. One of the heralding advantages of the Spheripol process, in combination with Ziegler-Natta catalysts, is its unique ability to produce polymer spheres directly, in the reactor. Propylene polymerisation leading to the formation of polypropylene homopolymer is schematically, described in the process flow diagram in Fig. 1.

It mainly, consists of the propylene storage drum, the loop reactors, the scrubbers to strip propylene from product mixture, the flash drum, the gas filter, the steamer, the dryer, the hoppers and the extruder. At the heart of the polypropylene production process is the loop reactor in which polymerisation of propylene takes place [8]. The loop reactor is used due to the low cost, high heat transfer and maintenance of uniform temperature, pressure and catalyst distribution.

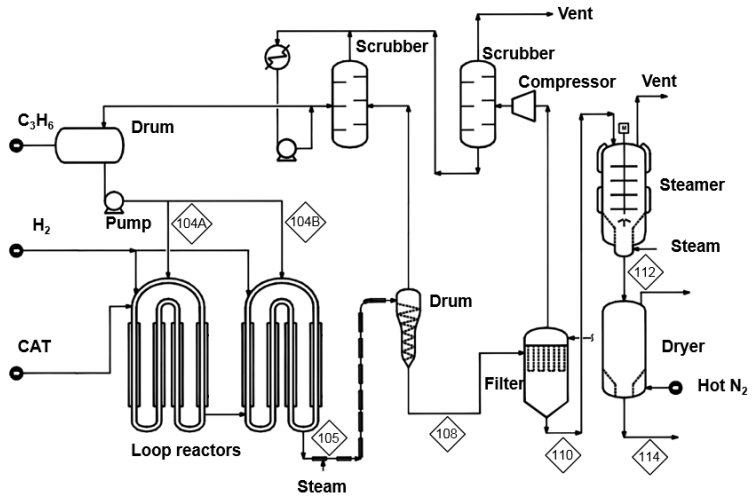

Fig. 1. Simplified Process Flow Diagram of Polypropylene Homopolymer Process [9].

3. Modelling and Simulation Approach

3.1. Model topology

One major point of this study is to work on the different levels of modelling abstraction of the polypropylene production process including:

- micro-scale modelling for chemical kinetics and reactor of propylene polymerisation in gPROMS
- macro-scale modelling for fractionation of slurry polymer in PRO/II
- multi-scale modelling for overall polypropylene production plant in the CAPE-OPEN framework.

The first level constituted polymer reactions in the loop reactor related to the kinetic model in which the best approach involved a detailed species balance. It also included the heat and population balance, as well as the polymer end-use properties. The second level also comprised of the modelling of process units for the feed preparation, as well as the fractionation of the slurry polymer from the reactor. The highest level of abstraction, the multi-scale model, then employed a consideration of the entire production of polypropylene from the feed and catalyst treatments through, the polymerisation reactors and the separations of monomer from polymer to the final part of the polymer treatment involving drying of the polymer product. The aforementioned levels were therefore, categorised into four major blocks as shown in Fig. 2.

The feed preparation was done in the feeding block and information was sent by streams to the reaction block which contains the reactor unit exported by CAPE-OPEN. Polymerisation calculations were executed here and the results sent onward to the treatment block for the separation and treatment of the polymer in the final stages.

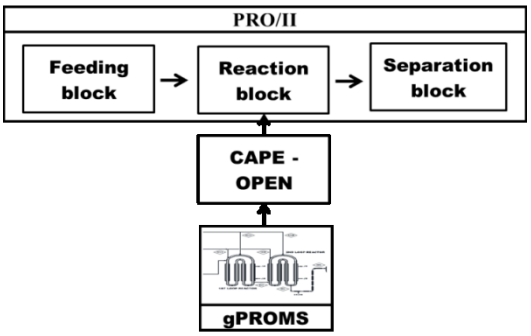

Fig. 2. The Modelling Topology for the Process Simulation.

3.2. Mathematical model of a loop reactor

Propylene polymerisation occurs in the loop reactor which is a closed tube with slurry flowing under high recycle rates driven by a recycling pump [10]. Hence, under the prevailing circumstance, it is possible to refer to this loop reactor as operating in the scheme of the CSTR with constant volume but variable reactor density. It is also assumed that due to high mixing, all state variables are uniform anywhere in the reactor and the catalyst particles are assumed to have equal activity. For a living or active chain of length i, the following mass balance equation can be formulated for these species [10].

$$V_R \frac{d[\phi]}{dt} = q_{in}[\phi]_{in} - q[\phi] + V_R S^m, \qquad \phi = P_i^*, P_i, M, C^*, H_2, AlR_3, C_d, \lambda_0 \tag{1}$$

where

$$S^m = \begin{cases} k_{iM}[C^*][M] - k_p[P_i^*][M] - \left(k_{trM}[M] + k_{trH}[H_2]^{0.5} + k_{trA}[AlR_3] + k_d\right)[P_i^*], \ i = 1; \ for \ P_i^* \\ k_P[M][P_{i-1}^*] - \left(k_{trH}[M] + k_{trH}[H_2]^{0.5} + k_{trA}[AlR_3] + k_p[M] + k_d\right)[P_i^*], \ i = 2..n-1; \ for \ P_i^* \\ \left(k_{trH}[M] + k_{trH}[H_2]^{0.5} + k_{trA}[AlR_3] + k_d\right)[P_i^*], \ for \ P_i \\ -k_{iM}[M][C^*] - (k_p + k_{trM})[M]\lambda_0, \ for \ M \\ (k_{trM}[M] + k_{trH}[H_2]^{0.5} + k_{trA}[AIR_3])\lambda_0 - k_{iM}[M][C^*] - k_d[C^*] - k_d\lambda_0, \ for \ C^* \\ -k_{trH}[H_2]^{0.5}\lambda_0, \ for \ H_2 \\ -k_{trA}[AIR_3]\lambda_0, \ for \ \mathrm{AlR_3} \\ k_d\lambda_0 + k_d[C^*], \ for \ \mathrm{C}_d \\ k_{iM}[C^*][M] - \left(k_{trM}[M] + k_{trH}[H_2]^{0.5} + k_{trA}[AIR_3] + k_d\right)\lambda_0, \ for \ \lambda_0 \end{cases} \tag{2}$$

Energy balance of the reactor constituents is given as [3]:

$$V_R \rho_s C_p \frac{dT}{dt} = f^{in} C_p^{in} T^{in} - f^{out} C_p T - UA\left(T - T^j\right) + V_R S^e \tag{3}$$

$$S^e = (-\Delta H_r) r_p \tag{4}$$

Chen and Ray [11] consolidated much of the existing mechanisms in literature to arrive at a reaction composed of several reaction steps. The Ziegler-Natta catalyst is assumed to go through the common activation - polymerisation - decay pathway and finally the chain transfer reactions occur with hydrogen, monomer and AIR_3 [12]. The comprehensive kinetic scheme comprising of the reactions as stated are shown in Table 1.

Table 1. Kinetic Mechanism [3, 8, 10 and 11].

Reaction step	Kinetic constant, $k=k_0 \exp(-E/RT)$
Activation	
$C^* + M \xrightarrow{k_{iM}} P_1^*$	$k_{iM} = 4.97\times10^7 \exp(-5e4/RT)$
Propagation	
$P_1^* + M \xrightarrow{k_p} P_2^*$	$k_p = 4.97\times10^7 \exp(-5e4/RT)$
$P_1^* + M \xrightarrow{k_p} P_{i+1}^*$	
Transfer	
Transfer to monomer	
$P_1^* + M \xrightarrow{k_{trM}} P_i + C^*$	$k_{trM} = 6.16\times10^3 \exp(-5e4/RT)$
Transfer to hydrogen	
$P_1^* + H_2 \xrightarrow{k_{trH}} P_i + C^*$	$k_{trH} = 4.4\times10^6 \exp(-5e4/RT)$
Transfer to cocatalyst (AlR_3)	
$P_1^* + AIR_3 \xrightarrow{k_{trA}} P_i + C^*$	$k_{trA} = 7.04\times10^2 \exp(-5e4/RT)$
Deactivation	
$P_1^* \xrightarrow{k_d} P_i + C_d$	$k_d = 7.92\times10^3 \exp(-5e4/RT)$
$C^* \xrightarrow{k_d} C_d$	

3.3. Polymer properties

The method of moments is used to determine the average molecular weights. Using the basic polymer properties like the average molecular weights, the end-use properties of the polypropylene homopolymer can be predicted by means of empirical correlations. The following expressions elaborate the determination of molecular weight averages and their relationship with end-use properties.

Molecular weight moments for live and dead polymers [13]:

$$\lambda_k^* = \sum_{i=1}^{\text{max\_chain}} i^k P_i^* \quad ; \quad \lambda_k = \sum_{i=2}^{\text{max\_chain}} i^k P_i \tag{5}$$

Number and weight average molecular weight [13]:

$$\bar{M}_n = m_0 \frac{\lambda_1^* + \lambda_1}{\lambda_0^* + \lambda_0} \quad ; \quad \bar{M}_w = m_0 \frac{\lambda_2^* + \lambda_2}{\lambda_1^* + \lambda_1} \tag{6}$$

Melt flow index [14] and polydispersity index [15]:

$$MFI = a \cdot (\bar{M}_w)^b \; ; \; PDI = \frac{\bar{M}_w}{\bar{M}_n} \tag{7}$$

where a = 3.39×1022 and b= -3.92

Flexural modulus (stiffness) [16]

$$E_f = \frac{a_1}{Mw} + a_2 XS + a_3 \tag{8}$$

$a_1 = -1.45 \times 10^5$; $a_2 = -3.37 \times 10^{-2}$; $a_3 = 2.2530$ XS= 4.13 for homopolymer

4. Results and Discussion

The dynamic model was simulated with conditions from the reference [2] to validate the model. The simulation conditions for this study are illustrated in Table 2.

Table 2. Simulation Conditions for Multi-scale Model [9].

Variable	Value
Temperature	318 K
Pressure	38.2 bar
Mass flow rate	53,000 (kg/hr)
Mass fractions	
Propylene	0.904
Propane	0.095
Catalyst	6.15×10^{-5}
Hydrogen	3.72×10^{-5}
AlR_3	1.61×10^{-3}

4.1. Transformation of the chain length domain to sub-interval domain

For the purpose of simulation, the number of chains is to be in the finite domain. In this study, the maximum number of chains was assumed to be 10^6. Considering each chain number for the simulation in terms of array would, however increase the system size enormously and lead to an expensive computational cost. In avoiding this situation, a sub-interval concept, the transformation of the axis from chain domain into sub-interval domain was employed such that;

$$z_{CL} \in [1 \ldots Max_{CL}] \quad \mapsto \quad _{--} \in [1 \ldots NO_{SI}] \tag{9}$$

In this study, we used 100 sub-intervals in transformation of chain length axis of which maximum value is 10^6. It is also worth noting that using the uniform interval size for the whole domain will mislead the simulation especially considering the unequal distribution of chain length. As a remedy, the size of sub-interval was determined by log transformation such as;

$$z_I = \frac{\log(\alpha z_c + 1)}{\log(\alpha + 1)} \tag{10}$$

The results of the log transformation based on Eqs. (9) and (10) are shown in Fig. 3. Each sub-interval has a different interval size in chain length. As the sub-

interval domain (x-axis) increases, the corresponding chain length interval (y-axis) also increases, which implies the lesser resolution for higher chain length region. With this approach, accurate simulation can be carried out for the wider range of chain length without paying extensive computational cost as well as losing accuracy.

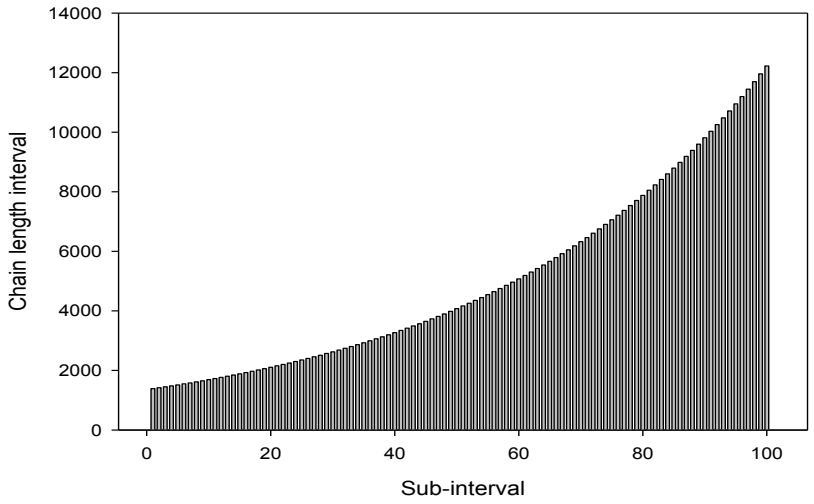

Fig. 3. The Result of the Log Transformation.

4.2. Validation of reactor model

The time transient profile of the monomer concentration of the simulation is compared with the results from the reference [2] as shown in Fig. 4. At steady state the monomer concentration for the simulation is 2.78 mol/L, which is 0.22mol/L below that of the reference data (3.0mol/L). In likewise manner, the profile for the conversion of monomers into polymer is also compared with the reference is illustrated with maximum conversion being attained at approximately, 0.7 after about 8,000s.

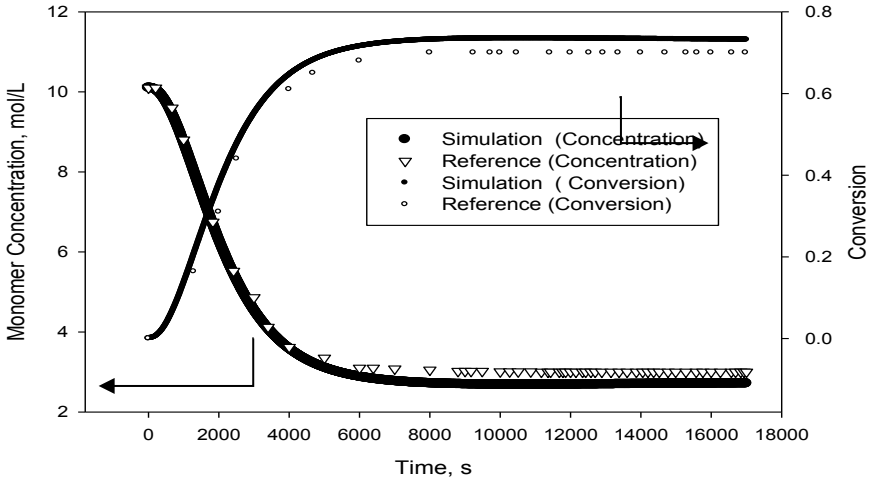

Fig. 4. Time Transient Profile of Monomer Concentration and Conversion.

Moreover, the behaviour of slurry temperature in the polymerisation process as a function of time is crucial for the management of heat in this system. This is because propylene evaporates at about 70^{o}C and hence, will disrupt the liquid-phase process if heat is not properly managed. The time transient profile for temperature in the reactor is illustrated in Fig. 5. It must however, be put on record that the unavailability of certain information required in executing the simulations in the study led to the marginal variations in the results reported between the reference and the work done in this paper.

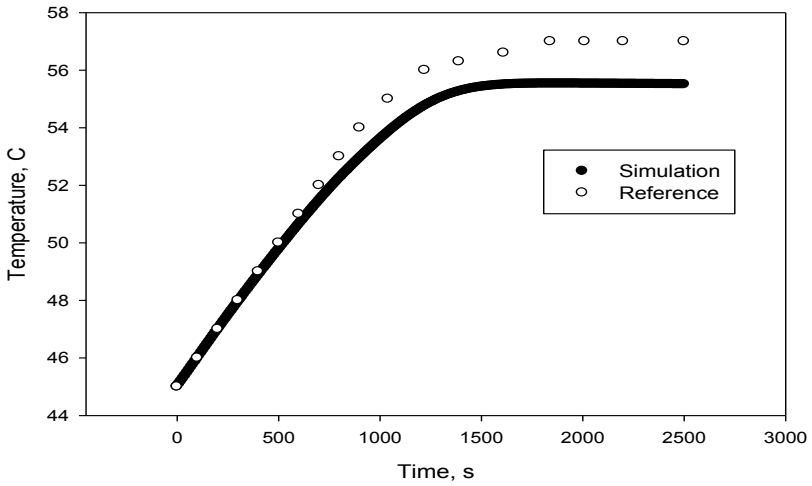

Fig. 5. Time Transient Profile of Temperature.

Values and decisions corresponding to such conditions were made guided by other literature documents and recommendations from experts acquainted with polymer simulations. These range from the choice of the maximum chain number through the number of intervals for molecular weight distribution to design conditions like the heat transfer area of the reactor. This is the reason for the marginal differences in the results of monomer concentration, conversion and temperature.

4.3. Result of steady state simulation of the overall plant using CAPE-OPEN

The multi-scale model with the exported reactor as a CAPE-OPEN unit is shown in Fig. 6. Selection of the appropriate thermodynamic methods is a crucial step in the execution of the simulation. This is because the process involves both pure components and polymer components which differ in properties. The involvement of the polypropylene polymer components led to the choice of the Flory-Huggins thermodynamic method. This method is useful for modelling polymer/solvent systems, especially if molecules are non-polar [6]. In addition, the Soave-Redlich-Kwong (SRK) equation of state was selected due to the involvement of pure components like H_2, N_2 and CO_2 in the system.

Table 3 describes the material balances of the occurring components in the process and their detail compositions, as well as the operating conditions at feed stream and some notable equipment on the flowsheet. From this table, it could be observed that the monomer is separated after the reaction by heating in the heat exchanger causing it to evaporate at 70^{o}C and the polymer is concentrated as you go downstream. Moreover, the polypropylene is sent to a steamer to deactivate the existing catalysts after which, it is further conveyed to the dryer where the moisture is removed. At this point, the stream composition as could be observed from Table 3 is about 99% propylene polymer.

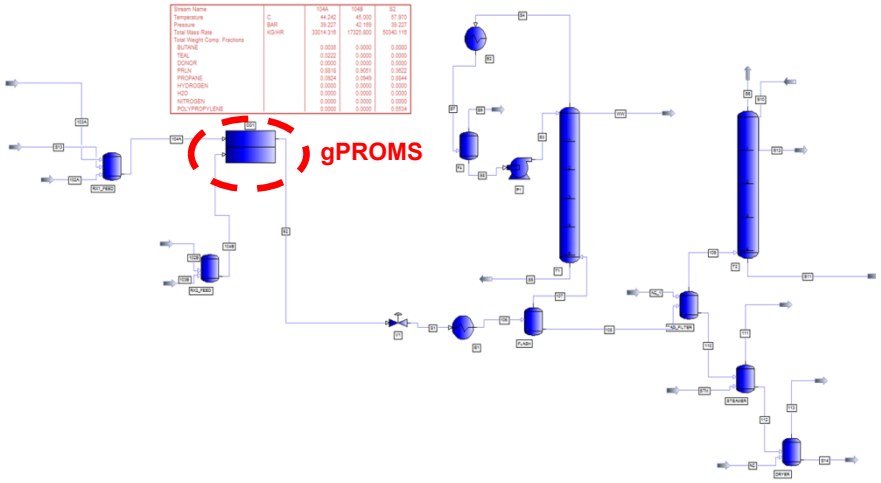

Fig. 6. Process Model in PRO/II with CAPE-OPEN.

Table 3. Material Balance of Chemical Components from the Simulation.

Stream Name	104A	104B	105	108	110	112	114
Description	Feed1	Feed2	Reactant from RX	Polymer from flash drum	Polymer from bag filter	polymer from steamer	Polymer from dryer
Temperature, C	44.2	45.0	55.0	70.0	65.0	104.3	89.0
Pressure, kg/cm^{2}g	39.0	42.0	39.0	2.0	0.5	0.2	0.1
Total Mass Rate, kg/h	33014.3	17325.8	50340.1	27352.6	27247.3	28091.4	27184.3
Weight Fractions							
Butane	0.00349	0.00000	0.00000	0.00000	0.00000	0.00000	0.00000
Teal	0.02224	0.00000	0.00000	0.00000	0.00000	0.00000	0.00000
Donor	0.00000	0.00000	0.00000	0.00000	0.00000	0.00000	0.00000
Propylene	0.88180	0.90507	0.45970	0.00660	0.00276	0.00004	0.00000
Propane	0.09245	0.09489	0.00054	0.00001	0.00000	0.00000	0.00000
Hydrogen	0.00004	0.00004	0.00000	0.00000	0.00000	0.00000	0.00000
Water	0.00000	0.00000	0.00000	0.00000	0.00000	0.03270	0.00042
Nitrogen	0.00000	0.00000	0.00000	0.00000	0.00002	0.00000	0.00004
Polypropylene	0.00000	0.00000	0.53976	0.99339	0.99723	0.96726	0.99954

In order to validate the process model, the results of the simulation were compared with a reference data [9]. The profile of the main feed component, propylene is first illustrated. This is in order to determine the level of conversion of the monomer into polymer and also understand the efficiency of the separation process after the reactor to remove residual propylene for recycling. A bar chart comparing the propylene mass fraction from simulation with that of the reference is shown in Fig. 7. Propylene being the main reactant is consumed in the polymerisation reaction as shown in Fig. 7 but some go unreacted and are vapourised in the heat exchanger after the reactor and are separated from the stream in the flash drum for recycling.

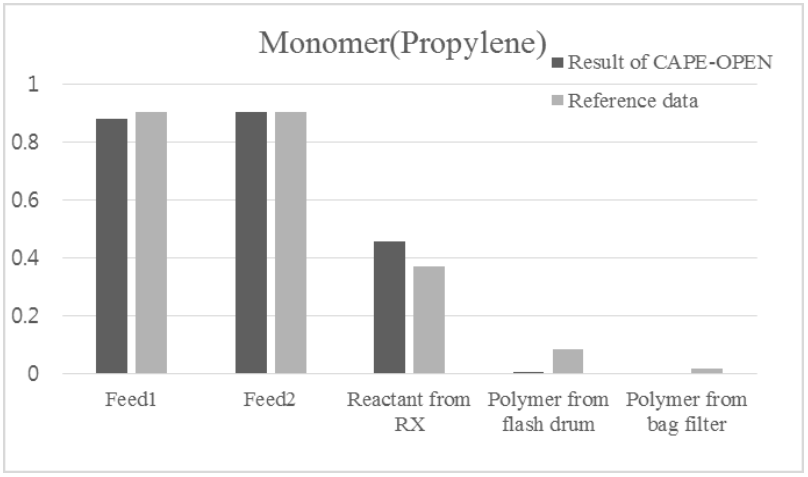

Fig. 7. Comparison of Propylene Mass Fraction.

This explains the significant reduction in propylene concentration from the flash drum onwards.

The next figure, Fig. 8, describes a comparison of the polypropylene polymer mass fractions from the CAPE-OPEN simulation with the reference.The marginal differences between the simulation and reference data that could be observed in Figs. 7 and 8 are caused by the numerical errors during simulation and the use of certain design and operating conditions which could not be found in the reference data for the simulation.

Furthermore, multi-scale simulation within this CAPE-OPEN framework allows the possibility of observing polymer end-use properties predicted in the reactor model. Hence, calculations made within the reactor model in using empirical correlations to predict the end-use properties could be seen as part of the simulation results in Table 4.

The polypropylene produced after this process has a molecular weight which is within the notable range of molecular weight of available for polypropylene grades as illustrated in Table 4. Meanwhile, the polydispersity of approximately, 2.3 is consistent to the range of polypropylene grades as illustrated. MFI is the commonest method of testing the flow characteristics of the polymer melt. By its definition, the MFI is an inverse measure of the melt viscosity of the polymer.

This property indeed controls the processability and spinability of the polymer resin formed [21]. The polypropylene formed has a MFI of 11.1g/10min, which is well within the range of polypropylene grades [18]. Also, the flexural modulus, which is proportional to the stiffness of the material is a very important property of the polymer. The value of the flexural modulus corresponds directly to the deformability, as well as the durability of the polymer. It is also inversely, proportional to the molecular weight of the polymer material [21]. The value obtained for the polypropylene formed in this process, 1.6GPa, is also within the range of the polypropylene grades as shown in Table 4.

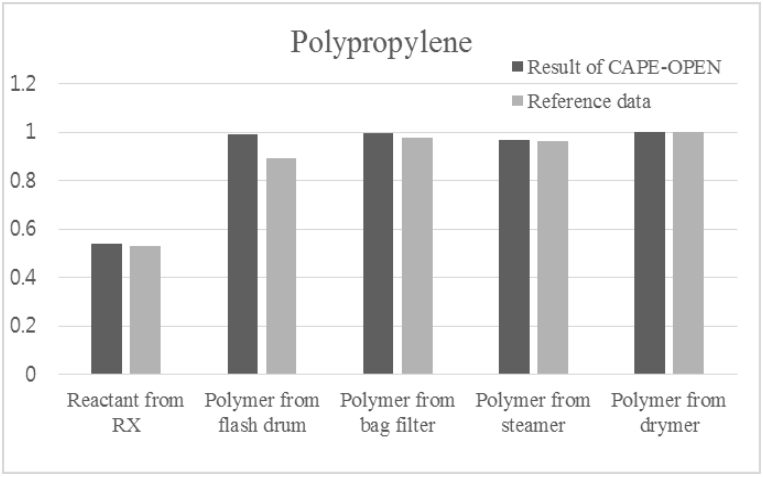

Fig. 8. Comparison of Polypropylene Mass Fraction.

Table 4. Polymer Properties.

Variable	Value	Typical value	Ref
Number average MW	137,567 g/mol	50,000-300,000	[17]
Weight average MW	322,483 g/mol	300,000-600,000	[17]
MFI	11.1 g/10min	0.50-70	[18]
$\mathbf{E_f}$	1.66GPa	1.5-2	[19, 20]
PDI	2.34	2-6	[17]

5. Conclusions

This work involved multi-scale modelling of the polypropylene production process taking the peculiar benefits of two process simulations software by simultaneous execution on a unified framework called CAPE-OPEN. The summary of the work done are the following:

- A dynamic model for the loop reactor on the basis of the polymerisation of propylene mechanism was developed considering the mass balance and polymerisation reactions.

- The model was validated with a reference data and was found to be consistent with a reasonable degree of error.
- The steady state form of the model was exported via the CAPE-OPEN interface to connect with other units on PRO/II environment to calculate the material balance and evaluate the process of polypropylene production. The fractionation units considered are polymer separation and treatment unit models including the steam jacket pipes, the degasser, the steamer and the dryer.
- Polymer end-use properties such as the MFI and PDI were also predicted by calculation of the molecular weight averages using the method of moments.

High level modelling and simulation of the reactor and the overall production process was achieved simultaneously, using the two powerful simulation software with a reduced modelling burden whilst maintaining accuracy and paying less computational cost.

Acknowledgement

This research is funded by the LINC Program of Hanbat National University (2014) and the authors would like to acknowledge for the assistance.

References

1. De Lucca, E.A.; Filho, R.M.; Melo, P.A.; and Pinto, J.C. (2008). Modelling and simulation of liquid phase propylene polymerisations in industrial loop reactors. *Macromolecules Symposium*, 271(1), 8-14.
2. Zacca, J.J.; and Ray, W.H. (1993). Modelling of the liquid phase polymerisation of olefins in loop reactors. *Chemical Engineering Science,* 48(22), 3743-3765.
3. Luo, Z.H.; Su, P.L.; and Wu, W. (2010). Industrial loop reactor for catalytic propylene polymerisation: dynamic modelling of emergency accidents. *Journal of Industrial Engineering Chemical Research,* 49(22), 11232–11243.
4. Neto, A.G.; and Pinto, J.C. (2001). Steady state modelling of slurry and bulk propylene polymerisations. *Chemical Engineering Science*, 56(13), 4043-4057.
5. gPROMS ModelBuilder® (2014). *Process Systems Enterprise*, London, United Kingdom.
6. Simsci PRO/II®. (2013). *Schneider Electric*, California, USA.
7. Spheripol LyondellBasell group. (2014). Licensed Polyolefin Technologies and Services. Retrieved July 7, 2014, from, http://www.lyondellbasell.com/Technology/LicensedTechnologies.
8. Alizadeh, M.; Mostoufia, N.; and Pourmahdian, S. (2004). Modelling of fluidized bed reactor of ethylene polymerisation. *Chemical Engineering Journal*, 97(1), 27-35.
9. Daelim Industrial Company Limited. (1998). *35 MTY polypropylene industrial plant*, Seoul. Republic of Korea

10. Luo, Z.H.; Zheng, Y.; Cao, Z.K.; Wen, S.H. (2007). Mathematical modelling of the molecular weight distribution of polypropylene produced in a loop reactor. *Polymer Engineering Science,* 47(10), 1643-1649.
11. Chen, C.M.; and Ray W.H. (1993). Polymerisation of olefins through heterogeneous catalysis; XI: gas phase sequential polymerisation kinetics. *Journal of Applied Polymer Science,* 49(9), 1573-1588.
12. Shaffer, W.K.A; and Ray, W.H. (1997). Polymerisation of olefins through heterogeneous catalysis; XXVII: A kinetic explanation for unusual effects. *Journal of Applied Polymer Science*, 65(6), 1053-1080.
13. Crowley, T.J.; and Choi, K.Y. (1997). Calculation of molecular weight distribution from molecular weight moments in free radical polymerisation. *Journal of Industrial Engineering Chemical Research,* 36(5), 1419-1423.
14. Bremner, T.; and Rudin, A. (1990). Melt flow index and molecular weight distributions of commercial thermoplastics. *Journal of Applied Polymer Science,* 41(7-8), 1617-1627.
15. Shamiri, A.; Hussain, M.A.; Mjalli, F.S.; and Mostoufi, N. (2010). Kinetic modelling of propylene homo-polymerisation in a gas-phase fluidized-bed reactor. *Chemical Engineering Journal*, 161(1-2), 240-249.
16. Latado, A.; Embirucu, M.; Mattos Netto, A.G.; and Pinto, J.C. (2001). Modelling of end-use properties of poly(propylene/ethylene) resins. *Polymer Testing*, 20(4), 419-439.
17. Anthony, L.A. (2003). *Plastics and the environment.* John Wiley & Sons Inc., New Jersey.
18. DSIR. (1998). Executive summary. Retrieved July 9, 2014, from www.dsir.gov.in/reports/techreps/tsr082.pdf
19. MatWeb. (2014). Material property data: flexural strength testing of plastics. Retrieved September 19, 2014, from http://www.matweb.com/reference/flexuralstrength.aspx
20. Smithers, Rapra. (2012). Mechanical properties of polymers. Retrieved September 21, 2014, from http://info.smithersrapra.com/downloads/chapters/Physical%20testing%20of%20plastics_chapter%201.pdf
21. Fatih Dogan. (2012). *Polypropylene.* InTech Books and Journals, Rijeka.